RSC Advances

ROYAL SOCIETY OF CHEMISTRY

www.rsc.org/advances

RSC Advances

ARTICLE

Characteristics of Graphene Quantum Dots Determined by Edge Structures: Three kinds of Dots Fabricated by Using Thermal Plasma Jet

Received 00th January 20xx,
Accepted 00th January 20xx

DOI: 10.1039/x0xx00000x

www.rsc.org/

Myung Woo Lee, Juhan Kim and Jung Sang Suh*

When a graphene sheet is cut along zigzag lines, carbene edges having two unshared valence electrons at each edge carbon atom are made, while along armchair lines carbyne edges having carbon triple bonds are made. Carbene and carbyne edges have polar and nonpolar characters, respectively. 90 degree corners are made when armchair and zigzag lines are encountered, while 120 degree corners are made when the same type lines are encountered. Therefore, hexagonal graphene quantum dots (GQDs) are made when the same type cutting lines are encountered, at all corners, while rectangular GQDs are made when different type cutting lines are encountered. We have fabricated three kinds of GQDs by a gas phase collision reaction using thermal plasma jet: Zigzag GQDs having only carbene edges were dispersed in polar solvents and had basically hexagonal shapes. Armchair GQDs having only carbyne edges were dispersed in nonpolar solvents and had also basically hexagonal shapes. Hybrid GQDs having both carbyne and carbene edges in each dot were dispersed in both polar and nonpolar solvents and had rectangular shapes. The photoluminescence and photoluminescence excitation spectra of hybrid GQDs responded to the combination of the spectra of zigzag and armchair GQDs.

Introduction

Graphene quantum dots (GQDs), which are graphene sheets smaller than 100 nm, possess strong edge effects and quantum confinement.[1] The former effects allow dispersion in solvents like ethanol, while graphene, which a pure carbon material, is not dispersible in common solvents. Graphene is a zero band gap semiconductor, which reduces its electronic and optoelectronic properties almost impossible to use for device applications.[2] However, the quantum confinement allows the bandgap of GQDs to be controlled by modulating their size.[3-5] GQDs could exhibit photoluminescence due to their band gap.[6-8] Their dispersible property, nonzero bandgap, chemical inertness, biocompatibility, low toxicity and strong photoluminescence make them excellent materials for applications such as nanoscale optics[9], electronic devices[10], bioimaging[11], OLEDs[12], fuel cells[13], photovoltaic devices[3], composites[14] and biosensors[15].

Controlled fabrication methods for stable graphene nanostructure provide a chance to investigate outstanding optical[16-22] and transport[23] properties of these structures. Both top-down and bottom-up methods have been used to prepare GQDs. Cut of graphene sheets[1] or graphene oxide sheets[24-27] or carbon fibers[10] or self-assembled block copolymer[28] or tattered graphite[29] or carbon black[30] or coal[31] corresponds to a top-down method, while self-assembling of aromatic carbons followed pyrolysis,[32] cyclodehydrogenation of polyphenylene precursors[33,34], microwave assisted hydrothermal method[12], tuning the carbonization degree of citric acid[35], and pulsed laser synthesis method from benzene[36] correspond to a

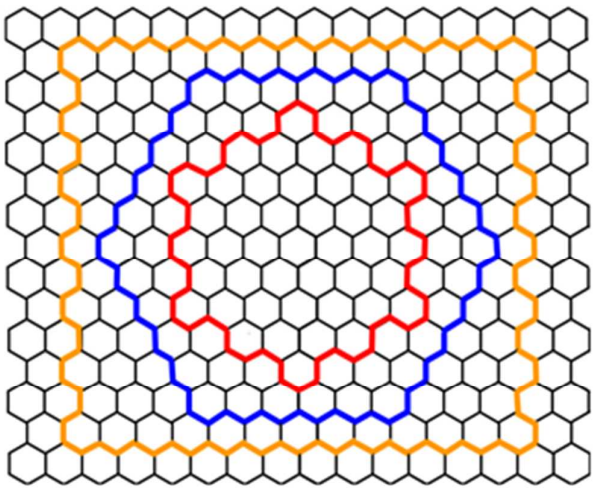

Fig 1. Model of three kinds of graphene quantum dots; red, blue and yellow are armchair, zigzag, and hybrid GQDs, respectively.

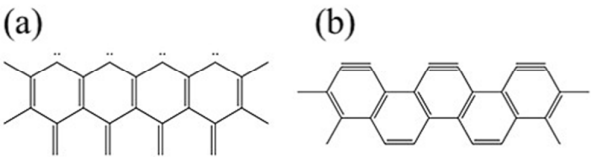

Fig 2. The edge structures of (a) carbene and (b) carbyne.

*Laboratory, Department of Chemistry, Seoul National University, Kwanakro 1, Kwanakgu, Seoul 151-747, Republic of Korea. *Corresponding author Tel: +82 2 880-7764 E-mail: jssuh@snu.ac.kr (Jung Sang Suh)*

Electronic Supplementary Information (ESI) available: [details of any supplementary information available should be included here]. See DOI: 10.1039/x0xx00000x

bottom-up method. Cage-opening of fullerenes[37] may be categorized as a third method. However, these methods have some drawbacks in the aspects of low-cost production, size-controllable fabrication, and mass production.

On a graphene sheet,[38] a 120 degree corner is made when two armchair lines or two zigzag lines are encountered, while a 90 degree corner is made when armchair and zigzag lines are encountered (see Figure 1). Therefore, in tailoring a graphene sheet, hexagonal GQDs are made when the same type cutting lines are encountered at all corners, while rectangular GQDs are made when different type cutting lines are encountered at all corners. When a graphene sheet is cut along an armchair line, carbon triple bonds are made at edges (see Figure 2). It is called carbyne, which may have a nonpolar characteristic due to carbon triple bonds at edges.[39] Along a zigzag line, two unshared valence electrons are made at each edge carbon atom. It is called carbene, which may have a polar characteristic due to lone pair electrons. Therefore, three kinds of GQDs could be distinguished by their shape and edge structure or dissolving property; two kinds of hexagonal GQDs dissolving either polar or nonpolar solvent, and rectangular GQDs dissolving in both polar and nonpolar solvents. For GQDs that can be dissolved in nonpolar solvent like cyclohexane and have hexagonal shapes could be named as armchair or nonpolar hexagonal (or simply nonpolar) GQDs. For GQDs that can be dissolved in polar solvent like water and have hexagonal shapes could be named as zigzag or polar hexagonal (or simply polar) GQDs. The GQDs that can be dissolved both in polar and nonpolar solvents and have rectangular shapes could be named as hybrid or amphoteric rectangular (or simply amphoteric) GQDs. Here, we have fabricated three kinds of GQDs by a gas phase collision reaction of carbon atoms using a thermal plasma jet system[40], and proved that the basic shape and dissolving property of our three kinds of GQDs are well agreed with those predicted from the model GQDs shown in Figure 1. For a 2.5 L/min injection rate of ethylene gas, the production rate of GQDs was about 4 g/hour. The relative abundance of armchair, zigzag and hybrid GQDs was 96.9, 2.7, and 0.4%, respectively.

Experimental

Carbon soot including GQDs was fabricated by using a thermal plasma system.[40] A carbon tube (10 cm in length; 2 cm in diameter) was attached to the anode, and ethylene gas was inserted continuously (2.5 L per min) as a carbon source into the torch using a gas flow meter (see Figure 3a). For extraction of GQDs, a small amount of carbon soot was scattered carefully on the surface of water that was contained in a vial, and then added cyclohexane carefully to minimize disturbance (see Figure 3b). After waiting for 48 h, two layers were separated without including undissolved carbon soot. For a further purification, cyclohexane was added into the separated aqueous phase, while water added into the organic phase. The volume ratio of water and cyclohexane was about 1:1. GQDs were analyzed by using a high-resolution transmission electron microscope (TEM; JEOL, JEM-3000F (300 kV)). The photoluminescence (PL) and photoluminescence excitation (PLE) spectra were obtained using a homemade spectrophotometer. Absolute quantum yield was measured by absolute PL quantum yield measurement system QE-1200 (OTSUKA Electronics). Atomic force microscopy (AFM) images were taken using a PSIA (XE-150) atomic force microscope. X-Ray Photoelectron Spectroscopy (XPS) analysis was performed using a PHI 5000 VersaProbe™ ULVAC system with an Al Kα X-ray source ($h\nu$ = 1486.6 eV), operated a 15kV and 20 mA beam, and HSA analyzer.

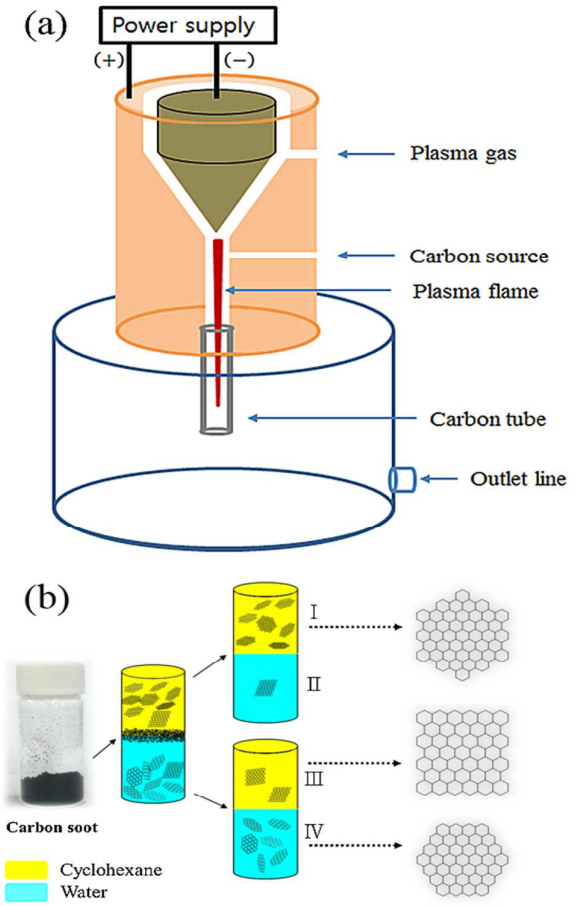

Fig 3. Schematics of (a) the thermal plasma jet system for production of carbon soot and (b) liquid-liquid extraction of three kinds of GQDs from carbon soot produced. Four solutions of I-IV are denoted as cyclohexane/cyclohexane, cyclohexane/water, water/cyclohexane, and water/water solutions, respectively.

Results and discussion

Figure 4 shows the low (a-c) and high (d-f) resolution TEM images of GQDs and (g) the fast Fourier transform (FFT) pattern of a GQD. GQDs were extracted from carbon soot produced, using liquid-liquid extraction method. Water and cyclohexane were used as polar and nonpolar solvents, respectively. It should be mentioned that the dominant species in carbon soot is onion type carbon materials, which is not dispersed without doing sonication.[40] Four solutions containing GQDs were denoted as cyclohexane/cyclohexane, cyclohexane/water, water/cyclohexane, and water/water solutions (see Figure 3b). The GQDs included in the cyclohexane/cyclohexane solution could be dissolved favorably in nonpolar solvent, while those included in the water/water

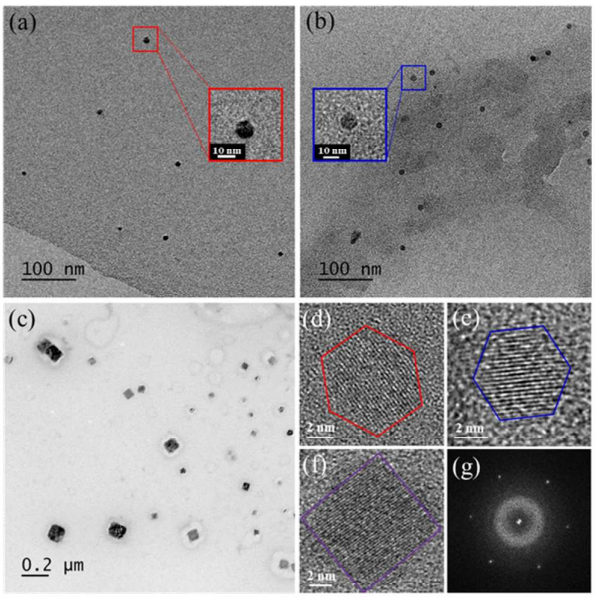

Fig 4. Low- and high-resolution TEM images of (a, d) armchair (or nonpolar hexagonal), (b, e) zigzag (or polar hexagonal) and (c, f) hybrid (or amphoteric rectangular) GQDs, and (g) the 2D FFT pattern of a zigzag GQD.

solution favorably in polar solvent. For GQDs included in the solutions of the cyclohexane/water or water/cyclohexane solution could be dissolved in both polar and nonpolar solvents. For the cyclohexane/water solution, we could not observe GQDs due to very low concentration even though the solution showed very weak fluorescence. GQDs shown in Figure 4a were obtained from the cyclohexane/cyclohexane solution. Their average size is about 13 nm (see Figure S1). Although the corners are not well developed, one can see clearly sides from all GQDs. They have basically hexagonal shapes (see Figure S4). GQDs shown in Figure 4b have been obtained from the water/water solution. The average size is about 11 nm (see Figure S2). They also have basically hexagonal shapes (see Figure S4). Some look like circular. This may be due to the fact that hexagonal shapes seem to be seen as circular shapes when the corners are not well developed. It should be mentioned that GQDs were made by collisions of carbon atoms. Therefore, the corners could not be made clearly as shown in Figure 1. GQDs shown in Figure 4c have rectangular shapes. They have been obtained from the water/cyclohexane solution. Their shape is relatively uniform as squares but their size has a large distribution. The largest one was about 300 nm, while the smallest one was about 15 nm. The large ones may be too big to be called as GQDs. The average size is about 53 nm (see Figure S3). It should be mentioned that the average of GQDs could be controlled by varying the length of carbon tube attached to anode. It is known that the average size of GQDs increases with increasing the length of carbon tube attached to anode.[40] In high-resolution TEM images of three kinds of GQDs, uniform lattice fringes are clearly seen. By AFM analysis, three kinds of GQDs are all single-layered. The height profiles of the lines in Figure S5-7 show that the thickness of the GQDs is less than 1 nm, which is in good agreement with the reported value for single-layered graphene.[41] The corresponding FFT patterns of GQDs are shown in Figure 4g and S8-10. They show a hexagonal pattern without any satellite spots. XPS was performed to determine the composition of three kinds of GQDs (see Figure S11). The measured spectra could be deconvoluted into four surface components, corresponding to sp^2 (C=C) at binding energy of 284.5 eV, sp^3 (C-C, and C-H) at 285.5 eV, C-OH at 286.6 eV, as well as O=C-OH at 288.6 eV. The bands corresponding to C-OH and O=C-OH were relatively weak. In principle, oxygen is not contained in our fabrication, since only Ar and ethylene gases have been added into a plasma system as the plasma gas and carbon source, respectively. Actually, according to the energy-dispersive X-ray spectroscopy (EDS) analysis of carbon soot including three kinds of GQDs, no oxygen is observed from carbon soot not exposed to air.[40] Therefore, oxygen of the hydroxyl and carboxyl groups might be included during the preparation process of XPS samples. It should be mentioned that H termination could take place because hydrogen atoms generated is twice of carbon atoms when ethylene molecules are decomposed. However, we could not get any information to be helpful in explaining the polar or nonpolar characters of GQDs or evidence of the H termination from the analysis of XPS or Raman spectra. This may be due to that the number of edge carbon or hydrogen atoms is relatively very small compared to the total number of carbon atoms of GQDs.

The shape and dissolving property of our three kinds of GQDs are well agreed with those predicted from the model GQDs (see Figure 1). Therefore, it is concluded that GQDs obtained from the cyclohexane/cyclohexane solution are armchair (or nonpolar hexagonal) GQDs having carbyne edges. GQDs obtained from the water/water solution are zigzag (or polar hexagonal) GQDs having carbene edges. GQDs obtained from the water/cyclohexane solution are hybrid (or amphoteric rectangular) GQDs having carbyne and carbene edges in each dot. Our conclusion is supported by the PL and PLE data. It is known that the PL of GQDs is determined by the edge structures.[1,39] Hybrid GQDs have both carbyne and carbene edges in each dot. Therefore, the PL spectra of hybrid GQDs may show the characteristic peaks corresponding to both armchair and zigzag GQDs.

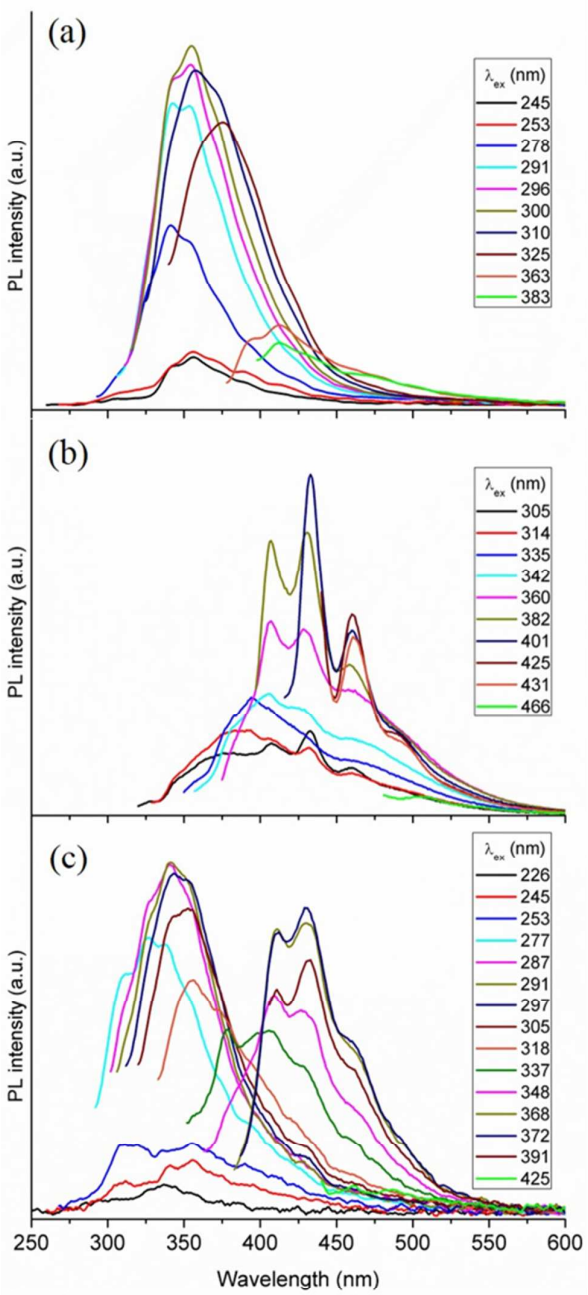

Fig 5. PL spectra of (a) zigzag (or polar hexagonal), (b) armchair (or nonpolar hexagonal), and (c) hybrid (or amphoteric rectangular) GQDs. Ethanol was the solvent for all samples. The legends are the excitation wavelengths.

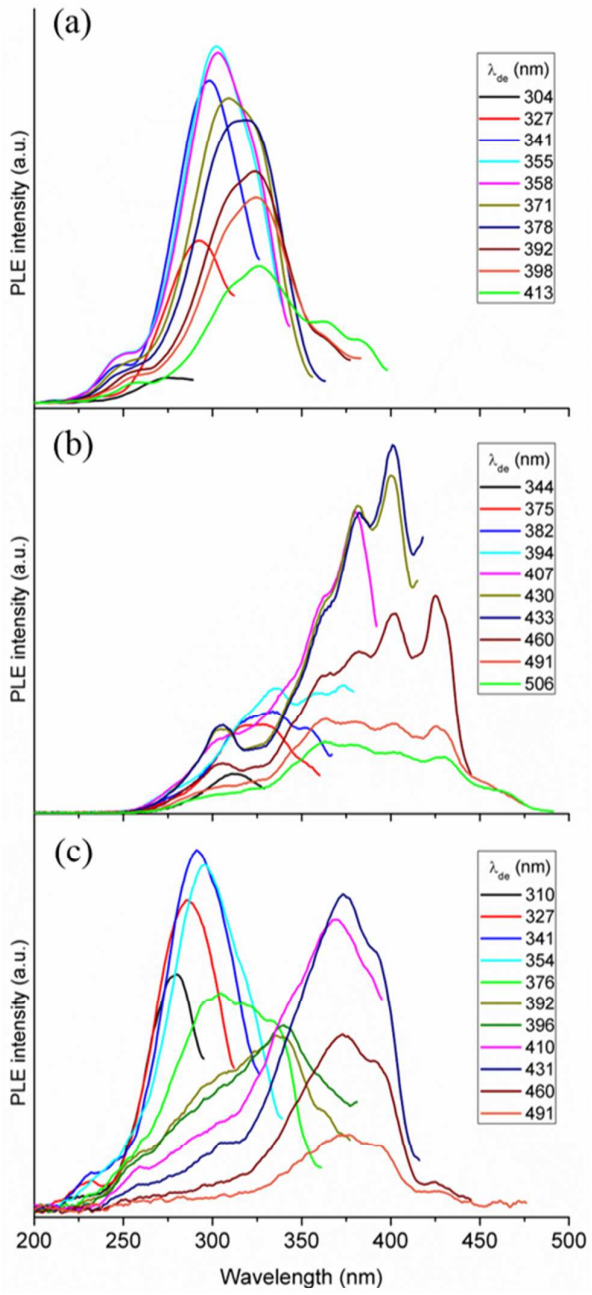

Fig 6. PLE spectra of (a) zigzag (or polar hexagonal), (b) armchair (or nonpolar hexagonal), and (c) hybrid (or amphoteric rectangular) GQDs. Ethanol was the solvent for all samples. The legends are the detection wavelengths.

The PL and PLE spectra of three kinds of GQDs are shown in Figures 5 and 6, respectively. [The UV-vis absorption spectra of armchair, zigzag, and hybrid GQD suspensions in ethanol are shown in Figure S13. Additional PL spectra are shown in Figure S12 with the luminescence pictures of GQD suspensions taken under 365 nm UV light.] In general shapes, the PL spectra of the hybrid (or amphoteric) GQDs seem to be the combination of the spectra of armchair (or nonpolar) and zigzag (or polar) hexagonal GQDs. A similar behavior is also observed in the PLE spectra. In the hybrid GQDs, the carbyne and carbene edges are not contacted directly except at four corners. It is known that the zigzag and armchair edges of graphene show different electronic and optical properties.[42,43] Therefore, one could assume that the carbyne and carbene edges of the hybrid GQDs do not affect strongly each other. If this assumption is true, the frequency of the peaks of hybrid GQDs should be matched to either that of zigzag or armchair GQDs and the intensity may simply correspond to the intensity sum of

armchair and zigzag GQDs. However, the relative intensity of some PL and PLE peaks of hybrid GQDs is significantly different from that of zigzag or armchair GQDs. For example, the PL spectrum measured by excitation with 318 or 325 nm is very strong for zigzag GQDs but medium for hybrid GQDs. For the PL spectrum measured by excitation with 403 nm light is very strong for armchair GQDs, while weak for hybrid GQDs. For the PLE spectrum measured by monitoring at 378 nm is very strong for zigzag GQDs, while medium for hybrid GQDs. In the PLE spectrum measured by monitoring at 460 nm, the peaks at 403 and 425 nm are strong for armchair GQDs, while those are weak for hybrid GQDs.

The frequency of the PL peaks of hybrid GQDs is well matched to either that of zigzag or armchair GQDs. The peak near 410 nm, whose λ_{max} is slightly different in each spectrum, of hybrid GQDs could be due to two close peaks at 412 nm for zigzag GQDs and at 408 nm for armchair GQDs. For the PLE spectra, several discrepancies in frequency are clearly observed. For example, for the PLE spectra measured by monitoring at 327 nm (3.79 eV), the strongest peak is at 291 nm (4.26 eV) for zigzag GQDs, while at 285 nm (4.35 eV) for hybrid GQDs. The λ_{max} is blue shifted from 291 to 285 nm. A similar shift, from 296 nm (4.19 eV) to 291 nm (4.26 eV), is observed in the PLE spectra measured by monitoring at 342 nm (3.64 eV). The strong PLE peaks near 372 nm (3.33 eV) of hybrid GQDs are not matched to any peak of armchair or zigzag GQDs. The λ_{max} is slightly shifted when the monitoring wavelength is changed. These peaks could be due to two peaks of armchair GQDs at 363 nm (3.42 eV) and 381 nm (3.25 eV). The former is weak, while the latter is relatively strong. The wavelength of 372 nm (3.33 eV) is corresponding to the middle of these two peaks in energy. Therefore, the peaks near 372 nm could be due to the two peaks at 363 and 381 nm, whose intensities were very similar to each other. The slightly different wavelength may be due to the factor that the λ_{max} is shifted toward the stronger peak when the relative intensity of the two peaks is not equal.

From our observations, it is concluded that the relative intensity of some PL and PLE peaks of hybrid GQDs is significantly different from that of armchair or zigzag GQDs. However, the frequency of the PL peaks is well matched to that of zigzag or armchair GQDs. For some PLE peaks, the frequency corresponding to roughly the vibrational energy of the excited state is shifted. By the theoretical calculation, there are seven energy levels for both carbyne and carbene, and the HOMO level is singlet for carbyne, while triplet for carbene.[39] The peak intensity is determined by the vibrational overlap integral.[44,45] By the Frank-Condon principle, the vibrational overlap integral could be changed when the upper or ground potential curve is displaced. When the potential curve is displaced, the absorption frequency is also changed in a vertical transition. Since no significant discrepancy in the PL frequency is observed, it is concluded that the electronic structure of armchair edges of hybrid GQDs is very similar to that of armchair GQDs and that of zigzag edges to that of zigzag GQDs. To show some significant discrepancy in relative intensity, the potential curves of hybrid GQDs should be slightly displaced from those of armchair or zigzag GQDs. Hybrid GQDs have both carbyne and carbene edges in each dot. Two unshared valence electrons exist at each carbon atom of zigzag edges, while carbon triple bonds exist at armchair edges. The former could act like electron donors and the latter as electron acceptors. Therefore, they could affect each other even though they are not contacted directly except four corners. This should be studied in detail.

The absolute quantum yields of armchair, zigzag and hybrid GQDs are summarized in Table 1. The quantum yield of hybrid GQDs is relatively very high as 25.3%. That of zigzag GQDs is 10.8%, which is the lowest. The PL intensity of zigzag GQDs is the highest when they are excited by a light of 300 nm (see Figure 5a). Due to limited light sources, the quantum yield of zigzag GQDs was measured by excitation with a 360 nm light. However, we could roughly figure out the actual quantum yield of zigzag GQDs. In the PL spectra of hybrid GQDs (see Figure 5c), the intensity is slightly higher at high energy region than low energy region. The high energy region is mainly contributed by carbene edges. This may mean that the quantum yield of zigzag GQDs having carbene edges is slightly higher than that of armchair GQDs having carbyne edges. Therefore, the actual quantum yield of zigzag GQDs might be higher than 17.4% of armchair GQDs. It is known that the quantum yield of GQDs decreases with increasing average size, while the PL and PLE spectra not change.[40]

Table 1. Absolute quantum yields of three types of GQDs

Types of Graphene Quantum Dots	λ_{ex} (nm)	Absorbance of the GQD solution	Quantum Yield (Q.Y)
Armchair GQDs	370	0.05	15.6%
	400	0.05	17.4%
Zigzag GQDs	360	0.05	10.8%
	370	0.05	8.6%
Hybrid GQDs	360	0.05	23.7%
	370	0.045	25.3%
9,10-diphenylantracene (blue dye)	370	0.05	91.3%

For a 2.5 L/min injection rate of ethylene gas, the production rate of carbon soot is 40 g/h.[40] GQDs are about 10% of the carbon soot produced, and the production rate of GQDs is about 4 g/hour.[40] We estimated the relative abundance of three kinds of GQDs by comparing their relative PL intensities. For measuring the PL spectra, the extracted solution of armchair GQDs was diluted 5 times, while the extracted solution of zigzag and hybrid GQDs was concentrated 4 times. To simplify, the quantum yield of three kinds GQDs was assumed to be equal. The relative abundance of armchair, zigzag and hybrid GQDs was calculated as 96.9, 2.7, and 0.4%, respectively.

Hybrid (or amphoteric rectangular) GQDs have carbyne and carbene edges in each dot. The shape of our hybrid GQDs is very uniform as squares (see Figure 4). Since it is known that the PL of GQDs is determined by the edge structures,[1,39] the PL and PLE spectra of hybrid GQDs will respond to the

combination of the spectra of zigzag and armchair GQDs. This is well agreed with our observations (see Figures 5 and 6). By model GQDs shown in Figure 1, an armchair GQD has only carbyne edges, while a zigzag GQD only carbene edges. The shape of armchair and zigzag GQDs is not uniform (see Figures 4 and S4). If carbene edges are partially formed in armchair GQDs or carbyne edges in zigzag GQDs, the peaks corresponding to minority should be observed. Nevertheless, they are not found in the PL and PLE spectra of armchair and zigzag GQDs (see Figures 5 and 6). This may mean that even though their shapes are not perfectly hexagonal, zigzag GQDs have only carbene edges and armchair GQDs have only carbyne edges. This could be possible only when the characteristics of edges do not change during growth of GQDs. Therefore, it is concluded that the seeds having both carbene and carbyne edges grow as hybrid GQDs, while the seeds having only carbene or carbyne edges grow as zigzag or armchair GQDs, respectively. Under our experimental conditions, it is very hard to collect the seeds of GQDs, because they could flow out of the chamber with Ar gas, which is the plasma gas, during fabrication. The growth mechanism of seeds should be studied in detail.

Our GQDs are made by a gas phase collision reaction. Therefore, our method can be categorized as a bottom-up method. Our method is a relatively low-cost process. Our thermal plasma system including a dc power supply is relatively inexpensive setup, and all chemicals are cheap. Also, the total electrical consumption is not substantial. The production rate of GQDs is about 4 g/hour. For a mass production of GQDs one could operate many plasma systems simultaneously. No oxygen is contained in our fabrication. Our GQDs have a relatively high quantum yields and can be dissolved in common solvents such as water, ethanol and cyclohexane. Also, the size of GQDs could be controlled by varying the length of carbon tube attached to anode. Therefore, they could be used in diverse fields such as nanoscale optical, bioimaging, and electronic devices.

Conclusions

We have fabricated three kinds of GQDs by a gas phase collision reaction of carbon atoms using a thermal plasma jet. They were extracted, using liquid-liquid extraction method, from carbon soot produced. Their shapes, dissolving properties in polar and nonpolar solvents, and PL data are well agreed with the three model GQDs, which are made when a graphene sheet is tailored along the zigzag or armchair lines. Armchair (or nonpolar hexagonal) GQDs, having carbyne edges, are well dispersed in nonpolar solvents like cyclohexane and have basically hexagonal shapes. Zigzag (or polar hexagonal) GQDs, having carbene edges, are well dispersed in polar solvents like water and have basically hexagonal shapes. Hybrid (or amphoteric GQDs are well dispersed in both polar and nonpolar solvents and have rectangular shapes. They have both carbyne and carbene edges in each dot. The PL and PLE spectra of hybrid GQDs contained almost all peaks of the armchair and zigzag GQDs. The absolute quantum yields of three kinds of GQDs are relatively very high. Hybrid GQDs show the highest yield of 25.3%. For a 2.5 L/min injection rate of ethylene gas, the production rate of GQDs is about 4 g/hour. The relative abundance of armchair, zigzag and hybrid GQDs is 96.9, 2.7, and 0.4%, respectively.

Acknowledgements

We thank G. L. Seol for help with TEM measurements. This work was supported by Basic Study program through the National Research Foundation of Korea funded by the Ministry of Education (NRF-2012R1A1A2003515), Nano R&D program through the National Research Foundation of Korea funded by the Ministry of Education, Science and Technology (20090082493), and the BK21 program.

Notes and references

1 L. A. Ponomarenko, F. Schedin, M. I. Katsnelson, R. Yang, E. W. Hill, K. S. Novoselov and A. K. Geim. *Science* 2008, **320**, 356.
2 K. S. Novoselov, A. K. Geim, S. V. Morozov, D. Jiang, Y. Zhang, S. V. Dubonos and I. V. Grigorieva, A. A. Firsov. *Science* 2004, **306**, 666.
3 X. Yan, X. Cui, B. Li and L. Li. *Nano. Lett.* 2010, **10**, 1869.
4 S. Neubeck, L. A. Ponomarenko, F. Freitag, A. J. M. Giesbers, U. Zeitler, S. V. Morozov, P. Blake and A. K. Geim. *Small* 2010, **6,** 1469.
5 L. Li and X. Yan. *J. Phys, Chem. Lett.* 2010, **1**, 2572
6 M. Li, W. Wu, W. Ren, H. Cheng, N. Tang, W. Zhong and Y. Do. *Appl. Phys. Lett.* 2012, **101**, 103107.
7 S. Kim, S. W. Hwang, M.-K. Kim, D. Y. Shin, D. H. Shin, C. O. Kim, S. B. Yang, J. H. Park, E. Hwang, S.-H. Choi, G. Ko, S. Sim, C. Sone, H. J. Choi, S. Bae and B. H. Hong. *ACS Nano* 2012, **6**, 8203.
8 M. L. Mueller, X. Yan, J. A. McGuire and L. Li. *Nano. Lett.* 2010, **10**, 2679.
9 K. A. Ritter and J. W. Lyding. *Nat. Mater.* 2009, **8**, 235.
10 V. Gupta, N. Chaudhary, R. Srivastava, G. D. Sharma, R. Bhardwaj and S. Chand. *J. Am. Chem. Soc.* 2011, **133**, 9960.
11 S. Zhu, J. Zhang, C. Qiao, S. Tang, Y. Li, W. Yuan, B. Li, L. Tian, F. Liu, R. Hu,H. Gao, H. Wei, H. Zhang, H. Sun, B. Yang. 2011, **47**, 6858.
12 L. Tang, R. Ji, X. Cao, J. Lin, H. Jiang, X. Li, K.S. Teng, C.M. Luk, S. Zeng, J. Hao, S.P. Lau. ACS Nano 2012, **6**, 5102.
13 L. Yan, Y. Zhao, H. Cheng, Y. Hu, G. Shi, L. Dai, L. Qu. J. Am. Chem. Soc. 2012, **134**, 15.
14 N. Jingjing, G. Hui, T. Wanfa. Prog. Chem. 2014, **26**, 270.
15 H. Sun, L. Wu, W. Wei, X. Qu. Mater. Today 2013, 16, 433.
16 D. Prezzi, D. Varsano, A. Ruini, A. Marini and E. Molinari. *Phys. Rev. B* 2008, **77**, 041404.
17 L. Yang, M. L. Cohen and S. G. Louie. *Nano. Lett.* 2007, **7**, 3112.
18 L. Yang, M. L. Cohen and S. G. Louie. *Phys. Rev. Lett.* 2008, **101**, 186401.
19 X. Zhu and H. Su. *J. Phys. Chem. C* 2010, **114**, 17257.
20 H. Hsu and L. E. Reichl. *Phys. Rev. B* 2007, **76**, 045418.
21 M. O. Goerbig, J. N. Fuchs, K. Kechedzhi and V. I. Fal'ko. *Phys. Rev. Lett.* 2007, **99**, 087402.
22 V. P, Gusynin, S. G. Sharapov and J. P. Carbotte. *Phys. Rev. Lett.* 2007, **98**, 157402.
23 B. Ozyilmaz, P. Jarillo-Herrero, D. Efetov, D. A. Abanin, L. S. Levitov and P. Kim. *Phys. Rev. Lett.* 2007, **99**, 166804.
24 D. Y. Pan, J. C. Zhang, Z. Li and M. H. Wu. *Adv. Mater.* 2010, **22**, 734.
25 J. H. Shen, Y. H. Zhu, C. Chen, X. L. Yang and C. Z. Li. *Chem. Commun.* 2011, **47**, 2580.
26 Y. Li, Y. Hu, Y. Zhao, G. Q. Shi, L. Deng, Y. B. Hou and L. Qu. *Adv. Mater*. 2011, **23**, 776.
27 J. Luo, L. J. Cote, V. C. Tung, A. T. L. Tan, P. E. Goins, J. Wu and J. Huang. *J. Am. Chem. Soc.* 2010, **132**, 17667.

28 J. Lee, K. Kim, W. I. Park, B.-H. Kim, J. H. Park, T.-H. Kim, S. Bong, C.-H. Kim, G. Chae, M. Jun, Y. Hwang, Y. S. Jung and S. Jeon. *Nano. Lett.* 2012, **12**, 6078.
29 W. Kwon, Y.-H. Kim, C.-L. Lee, M. Lee, H. C. Choi, T.-W. Lee and S.-W. Rhee. *Nano. Lett.* 2014, **14**, 1306.
30 Y. Dong, C. Chen, X. Zheng, L. Gao, Z. Cui, H. Yang, C. Guo, Y. Chi and C. M. Li. *J. Mater. Chem.* 2010, **22**, 8764.
31 R. Ye, C. Xiang, J. Lin, Z. Peng, K. Huang, Z. Yan, N. P. Cook, E. L. G. Samuel, C.-C. Hwang, G. Ruan, G. Ceriotti, A.-R. O. Raji, A. A. Marti and J. M. Tour. *Nat. Commun.* 2013, **4**, 2943.
32 R. Liu, D. Wu, X. Feng and K. Müllen. *J. Am. Chem. Soc.* 2011, **133**, 15221.
33 J. S. Wu, W. Pisula and K. Müllen. *Chem. Rev.* 2007, **107,** 718.
34 X. Yan, X. Cui and L. S. Li. *J. Am. Chem. Soc.* 2010, **132**, 5944.
35 Y. Dong, J. Shao, C. Chen, H. Li, R. Wang, Y. Chi, X. Li and G. Chen. *Carbon* 2012, **50**, 4738.
36 K. Habiba, V. I. Makarov, J. Avalos, M. J. F. Guinel, B. R. Weiner and G. Morell. *Carbon* 2013, **64**, 341.
37 J. Lu, P. S. E. Yeo, C. K. Gan, P. Wu and K. P. Loh. *Nat. Nanotechnol.* 2011, **6**, 247.
38 A. K. Geim and K. S. Novoselov. *Nat. Mater.* 2007, **6**, 183.
39 L. R. Radovoc and B. Bockrath. *J. Am. Chem. Soc.* 2005, **127,** 5917.
40 J. Kim and J. S. Suh. *ACS Nano* 2012, **8**, 4190.
41 A. Gupta, G. Chen, P. Joshi, S. Tadigadapa and P. C. Eklund. *Nano Lett*. 2006, **6**, 2667.
42 D. R. D. Costa, A. Chaves, M. Zarenia, J. M. Pereira Jr, G. A. Farias and F. M. Peeters. *Phys. Rev. B* 2014, **89**, 075418.
43 M. Grujic´, M. Zarenia, A. Chaves, M. Tadic´, G. A. Farias and F. M. Peeters. *Phys. Rev. B* 2011, 84, 205441.
44 T. Terasaka and M. Toshiki. *Chem. Phys. Lett.* 1981, **80**, 306.
45 E. U. Condon. *Phys. Rev.* 1928, **32**, 858.

Table of content

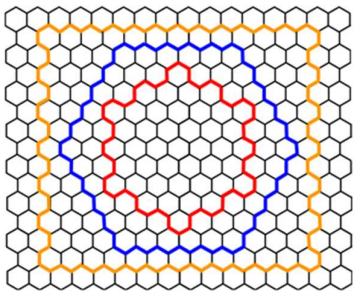

Model structures of three kinds of graphene quantum dots; armchair (red), zigzag (blue), and hybrid (yellow) GQDs.